HHS Public Access

Author manuscript

Arch Biochem Biophys. Author manuscript; available in PMC 2015 October 08.

Published in final edited form as:

Arch Biochem Biophys. 2013 September 1; 537(1): 31–38. doi:10.1016/j.abb.2013.06.001.

The aryl hydrocarbon receptor interacts with nuclear factor erythroid 2-related factor 2 to mediate induction of NAD(P)H: quinoneoxidoreductase 1 by 2,3,7,8-tetrachlorodibenzo-p-dioxin

Liping Wang[a,b,*], **Xiaoqing He**[c], **Grazyna D. Szklarz**[b], **Yongyi Bi**[a], **Yon Rojanasakul**[b], and **Qiang Ma**[c,*]

[a]Department of Occupational and Environmental Health, School of Public Health, Wuhan University, Wuhan 430071, China

[b]Department of Basic Pharmaceutical Sciences, School of Pharmacy, West Virginia University, USA

[c]Receptor Biology Laboratory, Toxicology and Molecular Biology Branch, Health Effects Laboratory Division, National Institute for Occupational Safety and Health, Centers for Disease Control and Prevention, Morgantown, WV 26505, USA

Abstract

NAD(P)H:quinoneoxidoreductase 1 (NQO1) belongs to a group of the aryl hydrocarbon receptor (AhR) battery of drug-metabolizing enzymes that are characteristically induced by both AhR agonists and nuclear factor erythroid 2-related factor 2 (Nrf2) activators. We have previously reported that induction of Nqo1 by the AhR agonist 2,3,7,8-tetrachlorodibenzo-p-dioxin (TCDD) in hepa1c1c7 cells involves Nrf2 (Ma et al., Biochem J 377, 205–213, 2004). Here we analyzed the molecular mechanism of induction. Induction required AhR and its DNA-binding partner Arnt because induction was not observed in AhR or Arnt-defective cells, but induction was restored upon reconstitution of the variant cells with functional AhR or Arnt. Induction also required Nrf2, as induction by benzo[a]pyrene was lost in the liver of Nrf2 knockout mice similarly to induction by butyl hydroxyanisol, demonstrating a cross-interaction between the AhR and Nrf2 pathways for induction in vivo. TCDD increased the protein level and induced the nuclear accumulation of Nrf2 with a delayed kinetics compared with activation of AhR. Chromatin immunoprecipitation revealed that TCDD recruited both AhR and Nrf2 to the Nqo1 promoter enhancer region containing a DRE and an ARE in time-dependent manners. Co-immunoprecipitation experiments revealed that, in addition to AhR-Arnt binding, TCDD induced an interaction between AhR and Nrf2 as well as Keap1. The findings reveal that TCDD induces multi protein complexes to mediate cross-interaction between the AhR and Nrf2 pathways, uncovering a novel mechanistic aspect of gene regulation by environmental chemicals through AhR and Nrf2.

[*]Corresponding authors. Address: 185 Donghu Road, Wuhan, Hubei 430071, China (L. Wang), Mailstop 3014, 1095 Willowdale Road, Morgantown, WV 26505, USA (Q. Ma). may21thwlp@163.com (L. Wang), qam1@cdc.gov (Q. Ma).

Disclaimer: The findings and conclusions in this report are those of the authors and do not necessarily represent the views of the National Institute for Occupational Safety and Health.

Keywords

Ah receptor; Nrf2; NQO1; TCDD; ARE; Cross-interaction

Introduction

2,3,7,8-Tetrachlorodibenzo-p-dioxin (TCDD)[1] is a ubiquitous environmental contaminant that elicits diverse, species-specific, xenobiotic metabolism effects including tumor promotion, teratogenesis, hepatoxicity, immunotoxicity, skin lesions, and disruption of endocrine functions [1,2]. TCDD as a potent agonist of the aryl hydrocarbon receptor (AhR) is best studied for induction of gene transcription. Studies on TCDD induction of CYP1A1, a highly inducible cytochrome P450 gene, have revealed a ligand-activated, receptor-mediated pathway for transcriptional gene regulation [3,4]. Induction is a necessary step for the metabolic activation of carcinogenic polycyclic aromatic hydrocarbons such as benzo[a]pyrene (B[a]P) by CYP1A1, because the enzyme is generally expressed at a low level in unstimulated cells in vivo and in vitro [5].

TCDD also induces a group of so-called “phase II” enzymes including NAD(P)H:quinoneoxidoreductase 1 (NQO1), glutathione S-transferase (GST) A1, UDP-glucuronocyltransferase (UGT) 1A1, 1A6, and 1A9, and aldehyde dehydrogenase (ALDH)3c [6,7]. Unlike CYP1A1, these enzymes are constitutively expressed in the liver and a range of other tissues and are inducible by both AhR agonists typified by TCDD and B[a]P and the nuclear factor erythroid 2-related factor 2 (Nrf2) activators including tert-butylhydroquinone (tBHQ, a phenolic antioxidant), sulforaphane (a phytochemical), triterpenoids (Michael reaction acceptors), and arsenic (a transition metal) [8]. Induction of the enzymes is believed to be an important mechanism for chemoprotection [9]. On the other hand, persistently elevated expression of the enzymes in tumors may promote tumor growth and drug resistance [10].

NQO1 (EC 1.6.99.2, DT-diaphorase) catalyzes the obligatory two-electron reduction of endogenous and environmental quinones and quinonoid compounds, such as benzo[a]pyrene-3,6-quinone, vitamin K, α-tocopherol, benzene quinone, and the anthraquinone anti-cancer agent mitomycin C [11,12]. Owing to its apparent inducibility and a role in chemoprotection, Nqo1 has served as a useful model for analyzing transcriptional regulation of the AhR battery of “chemoprotective” genes [13,14]. Induction of Nqo1 by TCDD is generally believed to be mediated through the AhR pathway similarly to induction of CYP1A1. In this scenario, TCDD-binding to AhR triggers the dissociation of AhR from an inhibitory cytoplasmic complex consisting of the AhR, two molecules of hsp90, and the AIP proteins. Activated AhR translocates into the nucleus and dimerizes with the Ah

[1]*Abbreviations used:* AhR, aryl hydrocarbon receptor; AhR-D, Ah receptor-deficient; ALDH, aldehyde dehydrogenase; ARE, antioxidant response element; Arnt, Ah receptor nuclear translocator; Arnt-D, Arnt-deficient; B[a]P, benzo[a]pyrene; BHA, butylatedhydroxyanisole; ChIP, chromatin immunoprecipitation; CHX, cycloheximide; DRE, dioxin response element; GST, glutathione S-transferase; Ho-1, hemeoxygenase 1; IB, immunoblotting; IP, immunoprecipitation; Keap1, Kelch-like erythroid cell-derived protein with CNC homology-associated protein 1; KO, knockout; NQO1, NAD(P)H:quinoneoxidoreductase; Nrf2, nuclear factor erythroid 2-related factor 2; ROS, reactive oxygen species; tBHQ, tert-butylhydroquinone; TCDD, 2,3,7,8-tetrachlorodibenzo-p-dioxin; UGT, UDP-glucuronosyltransferase; WT, wild-type.

receptor nuclear translocator (Arnt). The AhR-Arnt dimer binds to the dioxin response element(s) (DRE) located at the gene promoter to mediate transcription. On the other hand, induction of Nqo1 by Nrf2 activators involves a novel “dedepression” mechanism [15,16]. In unstimulated cells, Nrf2 is rapidly degraded through unibiquitination and proteasomal degradation controlled by the Keap1/Cul3 ubiquitin ligase. Nrf2 activators bind to reactive cysteine thiols of Keap1 and Nrf2 (coined “cysteine codes”) and, thereby, suppress Nrf2 degradation, leading to the activation and nuclear accumulation of Nrf2 protein. In the nucleus, Nrf2 dimerizes with a small Maf protein and the Nrf2/Maf dimer binds to an antioxidant response element(s) (ARE) at the Nqo1 promoter to control gene transcription.

Recent studies revealed that induction of Nqo1 by AhR agonists requires both AhR and Nrf2, suggesting an interaction between the two pathways in the mechanism of induction [17]. A cross-talk between AhR and Nrf2 may occur by at least two mechanisms. TCDD could increase the expression of Nrf2 mRNA and protein several folds through a functional DRE located in the promoter of Nrf2 [18]; in a reciprocal manner, Nrf2 activators stimulate AhR expression via several AREs within the promoter of AhR [19]. Given that Keap1 targets newly translated Nrf2 for ubiquitination and proteasomal degradation effectively, this mechanism of induction would require antagonizing repression of Nrf2 by Keap1 in order to keep newly synthesized Nrf2 from degradation. Alternatively, TCDD may stimulate a physical, protein–protein interaction between AhR and Nrf2 to increase the stability of Nrf2. Liganded AhR has been shown to interact with several transcription factors such as the estrogen and androgen receptors [20]. Furthermore, TCDD was found to induce a nuclear complex that binds specifically to a synthetic ARE sequence in vitro, but formation of the complex was preventedby antibodies against AhR [7]. It therefore seems possible that AhR associates with a protein complex that is bound to ARE for TCDD induction of Nqo1. However, the nature and the functional significance of this association remain unknown. It is also unclear whether TCDD increases Nrf2 binding to Nqo1 promoter to account for induction, because Nrf2 controls the basal expression of Nqo1 and, therefore, Nrf2 may influence Nqo1 induction by TCDD through its basal activity at the promoter [17].

Thus, there appears to be an interaction between AhR and Nrf2 in TCDD induction of Nqo1, Gsts, Ugts, and Aldhs at the promoters of the genes. In this paper, we show that TCDD stimulates Nrf2 binding to ARE and induces AhR interaction with Nrf2 by physical binding, both of which are necessary for induction of Nqo1 by TCDD.

Material and methods

Material

2,3,7,8-Tetrachlorodibenzo-p-dioxin (TCDD) was purchased from AccuStandard (New Haven, CT, U.S.A.). Benzo[a]pyrene (B[a]P), *tert*-butylhydroquinone (tBHQ), 3-*tert*-butyl-4-hydroxyanisol (BHA), dimethyl sulfoxide (DMSO), and corn oil were from Sigma (St. Louis, MO, U.S.A.). Antibodies against AhR were from BioMol (#SA-210-0100;Plymouth Meeting, PA). The monoclonal antibody against Arnt was from BD Biosciences (#611078; San Jose, CA). Antibodies against Nrf2 (#sc-722), Keap1 (#sc-15246), Lamin A (#sc-20680), and Actin (#sc-8432) were from Santa Cruz Biotechnology Inc. (Santa Cruz, CA).

Cell culture

Mouse hepa1c1c7 (wild-type, WT), AhR-defective variant (AhR-D, TAO), and Arnt-defective variant(Arnt-D, BP^{r}c1) cells were provided by Dr. J. P. Whitlock, Jr. (Stanford University) [21]. AhR-D cells express a low level of the AhR protein (~5% of the level in WT cells); whereas, Arnt-D cells express a normal level of AhR but is defective in CYP1A1 induction because liganded AhR fails to accumulate in the nucleus. The AhR-D cells expressing AhR, AhRR39A, or AhR515, and Arnt-D cells expressing Arnt, ArntR86A, or Arnt685 were originally from the laboratory of Dr. J. P. Whitlock, Jr. The cells were generated by using the MFG retroviral expression system as described elsewhere [22–24]. The cells were grown in α Minimal Essential Medium with 10% fetal bovine serum and 5% CO_2 at 37 °C. DMSO was used as a solvent control for TCDD and tBHQ treatments.

Animal treatment

Nrf2 knockout (KO) mice in which the Nrf2 gene was disrupted and non-functional were described elsewhere [17,25]. Nrf2 KO and WT mice in C57BL/6 background (male, 2 months old) were housed according to guidelines for animal care and use at National Institute for Occupational Safety and Health. Mice were barrier maintained with a light/dark cycle of 12 h at a constant temperature (22 °C) in HEPA-filtered, individually ventilated microisolator cages. Irradiated food and water were provided *ad libitum*. Bedding used was sterile Beta chips. Mice were treated with B[a]P by intraperitoneal injection at 80 mg/kg body weight once, or with BHA by intragastric administration at 400 mg/kg body weight on day 1 and day 3. Corn oil was used as the solvent control. Six mice were included for each genotype and treatment. Liver tissues were collected for preparation of total RNA and protein samples one day after B[a]P injection or 4 days after BHA treatment.

RNA preparation and real-time PCR

Total RNA was isolated from the mouse liver or cultured cells using the Qiagen total RNA isolation kit (Qiagen, Valencia, CA). The mRNA was reverse-transcribed into cDNA with a RNA reverse transcriptase. The cDNA samples were analyzed by real-time PCR performed on a Bio-Rad iCycler (Bio-Rad, Hercules, CA) using SYBR Green PCR Master Mix (Applied Biosystems, Foster City, CA) following standard procedures. In brief, for each reaction, the DNA template, forward and reverse primers (10 μM each), PCR Master Mix, and water were added to a final volume of 50 μl. Thermal cycling was performed as follows: 95 °C for 3 min as initial denaturing, followed by 45 cycles of 94 °C for 30 s, 60 °C for 30 s, and 72 °C for 60 s, and a final extension at 72 °C for 2 min. Threshold cycles (C_T values) were determined using iCycler IQ software (Bio-Rad). Relative cDNA amounts were calculated from C_T values for each sample by interpolating into a standard curve obtained from a series of dilution of a DNA sample that has a high expression level for the gene of interest. The PCR reactions for the standard curve were run under the same condition and with the same primers as those for the unknown samples. In this manner, the cDNA amounts were determined over a linear range with a slope characteristic of a particular gene fragment under the experimental condition. The sequences of the primer sets used for real-time PCR were as follows: Cyp1a1, forward 5′ GACTCTCCTGACTGGGCAGA and reverse 5′ CCCCCTCTTTTGCTGTCATA; Nqo1, forward 5′ AACGGGAAGATGTGGAGATG and

reverse 5′ CGCAGTAGATGCCAGTCAAA; and Ho-1, forward 5′ GAGCAGAACCAGCCTGAACTA and reverse 5′ GGTACAAGGAAGCCATCACCA. To visualize the results, real-time PCR was stopped at cycles at which differences between treatments and controls became apparent, and the cDNAs amplified were fractionated on a 1% agarose gel followed by staining with ethidium bromide for detection under the UV light.

Cell fractionation

Nuclear and cytoplasmic fractions were prepared using the Nuclei EZ PREP reagents from Sigma. Briefly, cells at 90% confluency in 10-cm dishes were washed with ice-cold phosphate buffered saline (PBS) and lysed with ice-cold Nuclei EZ PREP lysis buffer containing protease and phosphatase inhibitors (1 mM phenylmethylsulfonyl fluoride, 1 mM Na_3VO_4, 1 mM NaF, and 1 μg/ml of aprotinin, leupeptin, and pepstatin A each; all added immediately before use). The cell lysate was centrifuged at 500*g* for 5 min at 4 °C to prepare nuclei (pellet fraction) and cytosol (supernatant fraction). Nuclei pellets were washed once with the lysis buffer and resuspended in a radioimmune precipitation assay buffer (RIPA buffer, 50 mM Tris–HCl, pH 7.4, with 1% Nonidet P-40, 0.25% sodium deoxycholate, 1 mM EDTA; protease and phosphatase inhibitors were added as described above). The nuclear and cytoplasmic fractions were stored at −80 °C till use.

Immunoblotting (IB)

Cells were lysed on ice with a RIPA buffer containing protease and phosphatase inhibitors for 30 min. The cell lysate was sonicated briefly and was centrifuged at 14,000*g* for 20 min to remove cell debris. Cell lysate (10–20 μg each) was fractionated in 10% sodium dodecyl sulfate–polyacrylamide gel electrophoresis (SDS–PAGE), transferred to polyviinglidene difluoride membranes (Bio-Rad, Hercules, CA) and blocked with 5% nonfat milk in PBS plus 0.05% Tween-20. The membrane was blotted with a primary antibody at 4 °C for overnight with shaking, followed by incubation with the horseradish peroxidase-conjugated secondary antibody for 1 h at room temperature. Protein bands were visualized using enhanced chemiluminescence detection reagents from Amersham Biosciences (Pisctaway, NJ). Actin was blotted as loading control.

Co-immunoprecipitation

For immunoprecipitation (IP), cell lysates or cell fractions were pre-cleared with protein G-agarose (Invitrogen) for 1 h at 4 °C, followed by incubation with IP antibodies at 4 °C overnight with shaking. Immune complexes were precipitated by incubation with protein G-agarose at 4 °C for 1 h and a brief centrifugation. The precipitates were washed extensively with PBS plus 0.05% Tween 20 and were subjected to fractionation by SDS–PAGE. Protein bands were detected by immunoblotting with specific antibodies as specified in figure legends. Data shown were representatives from two to three separate experiments.

Chromatin immunoprecipitation (ChIP) assay

Hepa1c1c7 cells were grown in a 10-cm dish to reach 90% confluence. The cells were treated for 5 h. ChIP assay was performed as described previously with modifications [26].

Briefly, DNA–proteins were cross-linked by incubation of the cells with 1% formaldehyde at 37 °C for 10 min. Excess formaldehyde was quenched with 0.125 Mglycine. The cells were collected in 1 ml of a lysis buffer (5 mM Pipes at pH8.0 with 85 mM KCl, 0.5% IGEPAL CA-630, and proteinase inhibitors). The nuclei were pelleted by centrifugation, washed, and re-suspended in the nuclei lysis buffer. DNA was sonicated to an average size of 200–1000 bp. Sheared chromatin was diluted in an IP dilution buffer (0.01% SDS, 0.1% Triton X-100, 1.2 mM EDTA, and 16.7 mM Tris/HCl at pH 8.0 with 167 mM NaCl) pre-cleared with protein G and salmon sperm DNA. Immunoprecipitation was performed with rabbit anti-mouse Nrf2 or AhR antibodies or a normal rabbit IgG (as control for IgG). The immune complex was reverse cross-linked by incubation with 5 M NaCl at 65 °C overnight. The DNA samples were purified and amplified by real-time PCR following standard procedures. Threshold cycles (C_T values) were determined using the iCycler IQ software (Bio-Rad). Real time PCR results were normalized using C_T values with 1% of input as an internal control. Relative DNA amounts were calculated from C_T values as described above under *RNA preparation and real-time PCR*.

Primer sets used for real-time PCR were as follows: *Nqo1* ARE forward, 5′ GCAGTTTCTAAGAGCAGAACG, and reverse, 5′ GTAGATTAGTCCTCACTCAGCCG; Nqo1 coding region forward, 5′ AACGGGAAGATGTGGAGATG, and reverse, 5′ CGCAGTAGATGCCAGTCAAA. The ChIP assay was routinely performed with two types of negative controls: (1) normal IgG from the same species as that of each immunoprecipitation antibody and (2) primers specific for the coding region of *Nqo1*.

Data quantification and statistical analysis

Statistical analysis was performed with one way ANOVA followed by *t*-test using the Graphpad Prism program (Graphpad Software, San Diego, CA).

Results

AhR agonists induce Nqo1 via AhR, Arnt, and Nrf2

Previous studies suggest that TCDD induction of Nqo1 requires both AhR and Nrf2. Here we provide further detailed characterization of dependence on AhR, Arnt, and Nrf2. We first used AhR-D and Arnt-D variant cells, and the variants reconstituted with AhR, Arnt, or their mutants; these variants and reconstituted cells have facilitated establishing the AhR-Arnt pathway for TCDD induction of CYP1A1. As positive control, induction of CYP1A1 in the cells was characterized (Fig. 1A). Cyp1a1 mRNA expression in unstimulated WT, AhR-D, and Arnt-D cells was barely detectable as expected (lanes 1, 3, and11). The mRNA was highly induced by TCDD (1 nM, 4 h) in WT cells (Lane 2, ~16-fold). Induction was largely reduced in AhR-D variants (Lane 4) due to the low level of the AhR protein in the cells (about 5% of WT). Induction was totally lost in Arnt-D variants (lane 12) from defective translocation of liganded-AhR into the nucleus. Reconstitution of AhR-D with AhR fully restored induction (lane 6), but reconstitution with AhR mutants that are incapable of DNA-binding (AhRR39A, lanes 7 and 8) or transactivation (AhR515, lanes 9 and 10) failed to restore induction. Reconstitution of Arnt-D with Arnt rescued induction (lane 14), but reconstitution with an Arnt mutant incapable of DNA-binding (ArntR86A, lanes 15 and 16)

did not restore induction. Arnt685 lacks the Arnt transactivation domain that is not required for induction of Cyp1a1 in intact cells; therefore, reconstitution of Arnt-D with Arnt685 gave full induction (Lanes 17 and 18).

Nqo1 was constitutively expressed in hepa1c1c7 cells and was induced by TCDD by 2.9-fold (Fig. 1B, lanes 1 and 2). Similarly to induction of Cyp1a1, induction of Nqo1 by TCDD was largely reduced in AhR-D cells (lane 4) and was abolished in Arnt-D cells (lane 12). Reconstitution of AhR-D with AhR but not AhRR39A or AhR515, and Arnt-D with Arnt or Arnt685 but not ArntR86A, restored Nqo1 induction. Taken together, these results demonstrated that, although the fold of induction for Nqo1 was much lower than that for CYP1A1, induction of Nqo1 by TCDD was dependent upon the presence of functional AhR and Arnt proteins similarly to induction of CYP1A1.

We used Nrf2 KO mice to examine the impact of Nrf2 on Nqo1 induction by AhR agonists in mouse liver. In the WT mouse liver, Cyp1a1 was shown to be expressed at a very low level (Fig. 2A, lane 1) and it was induced by the AhR agonist B[a]P by 14-fold (lane 2), but was not induced by Nrf2 activator BHA (lane 3). Induction by B[a]P was observed in the Nrf2 KO liver but induction was reduced by 36% compared with WT (compare lane 5 with lane 2), suggesting a mild effect of Nrf2 KO on Cyp1a1 induction by B[a]P. For Nqo1, constitutive expression of the gene was readily detected in the WT mouse liver (Fig. 2B, lane 1) but the expression was reduced by 2.5-fold in the Nrf2 KO liver (compare lane 4 with lane 1), which reflects a critical role of Nrf2 in mediating the basal expression of Nqo1. Both B[a]P and BHA induced Nqo1 in the WT liver (Fig. 2B, lanes 2 and 3). BHA failed to induce the gene in the Nrf2 KO liver (Fig. 2B, lane 5) and induction by B[a]P was also lost (lane 6). Taken together, the results demonstrated that, in addition to controlling the basal expression of Nqo1 and induction by Nrf2 activators, Nrf2 is required for induction of the gene by B[a]P in vivo. This conclusion is in an agreement with the results obtained from primary embryonic fibroblasts of Nrf2 WT and KO mouse embryos reported previously [17].

TCDD promotes nuclear accumulation of Nrf2

In unstimulated cells, Nrf2 is rapidly degraded through ubiquitination-proteasomal degradation. Increasing the protein level of Nrf2 by stabilizing the protein is a major mechanism by which antioxidants and electrophiles activate Nrf2. The finding that Nrf2 plays a critical role in Nqo1 induction by AhR agonists both in vivo and in vitro raised a question of whether AhR agonists modulate the Nrf2 protein level. Fig. 3A shows that the Nrf2 protein was barely detectable in control cells (lane 1), but the protein amount was significantly increased by treatment with tBHQ (lane 5, 30 μM, 4 h). Treatment with TCDD (1 nM, 4 h) also increased the Nrf2 protein level, albeit, to a much less extent than induction with tBHQ (~50%, compare lane 3 with lane 5). Cycloheximide (CHX), a potent inhibitor of protein synthesis, reduced the basal level and blocked the induction of Nrf2 protein by either TCDD or tBHQ, demonstrating that Nrf2 is a labile protein (lanes 2, 4, and 6). We further validated these findings by using immunoprecipitation, in which Nrf2 was immunoprecipitated from treated cells before immunoblotting (Fig. 3B). As shown, tBHQ

and, to a lesser extent, TCDD increased the amount of the Nrf2 protein immunoprecipitated from the cells by antibodies specific for Nrf2.

We then examined the nuclear accumulation of Nrf2 in comparison with that of AhR. Nuclear fractions were isolated from cells before and after TCDD treatment at different time points. The nuclear fractions contain equal amount of Lamin A (a nuclear marker) but lack actin (a cytoplasmic marker) indicating the lack of cytoplasmic contamination (Fig. 4, panels 3 and 4). TCDD induced a rapid accumulation of AhR in the nucleus at 0.5 h after treatment, but the AhR protein level decreased at 4 h, possibly due to ligand-activated degradation of AhR in the nucleus (panel 2). TCDD also induced the accumulation of Nrf2 in the nucleus (panel 1). The increase of Nrf2 in the nucleus was observed at 1 h and the protein level did not decrease at 4 h after treatment. As a positive control, tBHQ (30 μM, 4 h) was shown to strongly increase the Nrf2 protein level (Panel 1, lane 6). Therefore, TCDD increased the protein level of Nrf2 and promoted the nuclear accumulation of the Nrf2 protein with an apparently delayed kinetics compared with that of the AhR protein.

TCDD recruits AhR and Nrf2 to the promoter of Nqo1 in vivo

The mouse and rat Nqo1 promoters contain an enhancer region with a DRE sequence and an ARE sequence, which are believed to mediate induction of Nrf2 by planar aromatic hydrocarbons and phenolic antioxidants, respectively [27]. We tested if TCDD increases Nrf2 binding to the enhancer in intact cells using the ChIP assay. As positive control, TCDD, but not tBHQ, was shown to increase the binding of AhR to the enhancer by 8-fold (Fig. 5A). As expected, the control serum did not affect AhR binding and no binding was detected with a primer pair specific for the Nqo1 coding region. A representative agarose gel electrophoresis of the bound DNA amplified by real-time PCR was shown in Fig. 5B where TCDD increased the binding of AhR to the Nqo1 enhancer (Lane 7).

Treatment with tBHQ increased Nrf2 binding to the enhancer by 15-fold (Fig. 6A). TCDD also increased the binding of Nrf2 by 9-fold. The control serum did not affect the binding by Nrf2 in cells treated with either tBHQ or TCDD. The serum control and the Nrf2 antibodies did not increase the binding of Nrf2 to the Nqo1 coding region. Fig. 6B showed similar results on agarose gel electrophoresis where lane 5 shows tBHQ-induced binding and lane 7 TCDD-induced binding.

We further characterized the kinetics of DNA-binding by ChIP assay. Treatment with tBHQ induced a time-dependent increase in the binding of Nrf2, but not AhR, to the enhancer as expected (Fig. 7A). On the other hand, TCDD induced a rapid increase in AhR binding that peaked at 2 h after treatment, but decreased significantly at 3, 4, and 5 h time points. TCDD increased the binding of Nrf2 to the enhancer at a slightly slower pace than that of for AhR; the binding peaked at 3 h and showed reduction at 4 and 5 h. Therefore, TCDD increased Nrf2 binding to Nqo1 enhancer, which has a similar but delayed kinetics compared with that for AhR binding.

TCDD induces AhR-Nrf2 and AhR-Keap1 interactions

TCDD is metabolically stable and does not convert to electrophiles in cells, which negates an interaction of TCDD with Keap1 cysteine thiols for Nrf2 activation. One potential

mechanism by which TCDD recruits Nrf2 to Nqo1 promoter is to induce oxidative stress in cells that activates Nrf2 through reactive oxygen species (ROS). We tested the possibility by examine the induction of hemeoxygenase 1 (Ho-1), a gene involved in heme catabolism and highly inducible by a variety of oxidative stress signals and electrophiles. Induction of Ho-1 by ROS and antioxidants involves the Nrf2/Keap1 and several other pathways [8]. Ho-1 mRNA is expressed at a low level but is highly induced by tBHQ (30 μM, 4 h), in hepa1c1c7 cells (Fig. 8, compare lane 3 with lane 1). CHX (10 μg/ml, 4 h) did not affect Ho-1 basal expression but inhibited induction by tBHQ significantly because it blocks the synthesis of Nrf2 to prevent Nrf2 activation by tBHQ (lanes 2 and 4). TCDD (1 nM, 4 h) or TCDD plus CHX did not induce Ho-1 (Lanes 5 and 6). The results indicate that TCDD did not induce a significant oxidative stress in the cells.

An alternative mechanism of Nrf2 activation involves TCDD activation of AhR that subsequently induces AhR-Nrf2 interaction and, thereby, stabilizes the Nrf2 protein. To test the possibility directly, co-immunoprecipitation was performed. As positive control, the interaction between AhR and Arnt was examined. Arnt was constitutively expressed in hepa1c1c7 cells with or without inducers (Fig. 9A, lanes 4–6). TCDD (1 nM, 4 h), but not tBHQ (30 μM, 4 h), induced AhR-Arntbinding (Compare lane 2 with 1 and 3). AhR was constitutively expressed in the cells (Fig. 9B, lane 4). The AhR protein level was not affected by tBHQ (Lane 5), but was decreased by TCDD (Lane 6); this result is consistent with a mechanism of ligand-activated degradation of AhR described previously [28]. Immunoprecipitation with anti-Nrf2 antibodies precipitated low but detectable amounts of AhR from control or tBHQ-treated cells (Fig. 9B, lanes 1 and 2), but TCDD significantly increased the amount of AhR co-immunoprecipitated with Nrf2 (lane 3). Thus, TCDD induced the formation of a complex containing both AhR and Nrf2, suggesting that AhR interacts with Nrf2 in the presence of TCDD.

Keap1 controls the ubiquitination and degradation of Nrf2. Therefore, we examined the interaction between AhR and Keap1. Keap1 was constitutively expressed in the cells and inducers did not change the Keap1 protein level (Fig. 9C, lanes 4–6). Treatment with TCDD significantly increased the amount of Keap1 co-immunoprecipitaed with anti-AhR antibodies compared with either control or tBHQ treatment (Compare lane 2 with lanes 1 and 3). Taken together, TCDD appeared to induce a number of protein–protein interactions between AhR and several other proteins in the AhR and Nrf2 pathways that were detected by co-immunoprecipitation. These include novel AhR-Nrf2 and AhR-Keap1 interactions in addition to the known AhR-Arnt binding.

Discussion

Induction of NQO1 has served as a useful model for understanding transcriptional regulation of a subgroup of the AhR battery of drub-metabolizing enzymes including NQO1, GSTs, UGTs, and ALDHs [8,13,29]. As a group, these enzymes exhibit a pattern of gene regulation, that is, they are constitutively expressed in the liver and a range of other tissues and cell lines, and are induced by both AhR agonists and Nrf2 activators. Induction of the genes is generally believed to play an important role in chemoprotection against cancer, chronic disease, and toxicity. Induction by planar aromatic hydrocarbons requires a DRE

sequence and induction by phenolic antioxidants requires an ARE enhancer. Recent studies uncovered an Nrf2-dependent, “dedepression” signaling pathway for ARE-dependent induction of the genes by antioxidants and electrophiles [8]. The molecular events governing Nqo1 induction by AhR agonists remain not well defined.

We have previously found that induction of Nqo1 by TCDD requires Nrf2, because inhibition of Nrf2 protein synthesis by cycloheximide blocked the induction and Nrf2 knockout fibroblasts were devoid of induction [17]. We extended these observations in the current study by demonstrating genetically that induction of Nqo1 by AhR agonists TCDD and B[a]P is dependent on the presence of functional AhR, Arnt, and Nrf2 both in vitro and in intact animals. The findings suggest a cross-interaction between the AhR-DRE pathway and the Nrf2-ARE pathway for Nqo1 induction by AhR agonists, which is a novel aspect of gene regulation through AhR.

Several mechanistic issues emerge from this model of AhR-Nrf2 cross-talk. It is known that Nrf2 mediates the basal expression of GstA1 and Nqo1 through AREs. Therefore, Nrf2 potentially influences TCDD induction of the genes through its basal activities at the promoters. In this scenario, TCDD does not necessarily affect the activity and cellular localization of the majority of Nrf2 protein. We found that the Nrf2 protein level was increased and Nrf2 was enriched in the nucleus upon stimulation with TCDD, indicating that Nrf2 was stabilized and activated. Moreover, binding of Nrf2 to the endogenous Nqo1 enhancer sequence containing a DRE and an ARE was largely increased as revealed by the ChIP assay. Therefore, not only did TCDD activate Nrf2, but also it increased Nrf2 activity at the Nqo1 promoter, which is fitting for increased transcription of the gene (Fig. 10).

The nuclear enrichment of Nrf2 induced by TCDD appeared to follow a delayed time course compared with that for activation of AhR (i.e., delayed ~½ h, Fig. 4). The AhR protein level decreased at 4 h, which is consistent with ligand-activated AhR degradation described previously [28]. The changes in nuclear Nrf2 and AhR protein levels correlated well with the amounts of AhR and Nrf2 recruited to Nqo1 enhancer (Fig. 7). These findings revealed potentially sequential events between AhR activation and Nrf2 activation and suggest an AhR-dependent mechanism of Nrf2 activation by TCDD.

TCDD activates AhR by binding to the ligand-binding pocket of the AhR-hsp90-AIP complex [3]. On the other hand, Nrf2 is known to be activated by antioxidants and electrophiles through binding with reactive cysteine thiols of Keap1 and Nrf2 [8]. However, TCDD is metabolically stable and is unlikely to convert to an electrophile(s) in cells. Therefore, it is perceived that TCDD does not activate Nrf2 by a mechanism(s) analogous to either TCDD-AhR binding or electrophile-Keap1/Nrf2 cysteine thiol binding.

Two mechanisms potentially account for Nrf2 activation by TCDD. First, TCDD may stimulate the production of reactive oxygen species that oxidize the reactive cysteine thiols of Keap1 and Nrf2 to inhibit Nrf2 ubiquitination and proteasomal degradation. However, at the low concentration of TCDD used (1 nM, 4 h), oxidative stress does not appear to be significantly increased in hepa1c1c7 cells because TCDD failed to stimulate the expression of Ho-1, which is a sensitive marker of oxidative stress (Fig. 8). Alternatively, TCDD may

bind and activate AhR first, and activated AhR then increases Nrf2 protein level, either by increasing Nrf2 gene transcription or by interacting with the Nrf2-Keap1 complex to inhibit Nrf2 degradation. In the former case, Nrf2 mRNA has been shown to be induced by TCDD via a DRE in the promoter of Nrf2 [18]; however, how the Nrf2 protein synthesized from induced mRNA escapes Keap1-mediated ubiquitination-proteasomal degradation remains unaddressed. Our findings support the latter scenario where TCDD-bound AhR activates Nrf2 by physical interactions with Nrf2 and Keap1 (Fig. 9). We provided the first evidence that TCDD stimulated an interaction between AhR and Nrf2 and between AhR and Keap1 in addition to the AhR-Arnt interaction. At a molecular level, liganded AhR may interact with Nrf2 or Keap1 directly as it does with Arnt; or, it may interact with the cytoplasmic Nrf2/Keap1/Cul3 complex to inhibit Nrf2 ubiquitination and degradation. TCDD may also stimulate the formation of a complex(s) of AhR, Arnt, and Nrf2 in the nucleus that binds to the DRE and ARE-containing enhancer of Nqo1 gene (Fig. 10). This AhR-dependent activation of Nrf2 by TCDD is consistent with the delayed activation and DNA-binding kinetics of Nrf2 compared with the kinetics of AhR activation (Figs. 3 and 7).

Although both DRE and ARE sequences have been identified as key regulatory, *cis*-acting factors for Nqo1, Gsta1, Ugt1a, and Aldh3c, the promoter structures and the DRE and ARE sequences vary from gene to gene to a certain extent. The mouse and rat Nqo1 enhancers contain the DRE and ARE within ~100 base pairs. Conceivably, this close-localization of the DRE and ARE would promote physical interactions among AhR, Arnt, and Nrf2 proteins at the promoter. It remains to be certain how the distance between DRE and ARE affects the binding of AhR and Nrf2 to enhancers of different genes in response to different inducers, and whether TCDD induces similar molecular activities at the enhancers of all DRE and ARE-containing genes. From this prospect, our findings provide an experimental model system to investigate the mode of action of TCDD in gene regulation involving AhR-Nrf2 cross-interaction in future studies.

The newly uncovered AhR-Nrf2 interaction for the induction of Nqo1 by AhR agonists occurs in the mouse liver (Fig. 2) and, thus, is potentially relevant to humans exposed to AhR agonists like the environmental halogenated aromatic hydrocarbons such as TCDD, the polycyclic aromatic hydrocarbons present in tobacco smoke and charcoal-broiled meat such as B[a]P, and certain clinical drugs such as the proton pump inhibitor omeprazole. The consequences of induction of the enzymes are likely to be context-dependent. For example, induction of the enzymes by B[a]P in normal cells may facilitate detoxification of carcinogens and, thereby, inhibit carcinogenesis, which counteracts with the effect of metabolic activation of B[a]P resulting from induction of Cyp1a enzymes. In tumor cells, induction of Nqo1 and Gsts may increase resistance of tumor cells to chemotherapeutic drugs as the drugs are easily metabolized by induced enzymes.

Acknowledgments

Grant support: The study was supported in part by a grant from the National Institute for Occupational Safety and Health USA (939ZXFF) to Q. Ma and by a grant from the National Nature Science Foundation China (810772276) to Y. Bi.

References

1. Birnbaum LS. Environ Health Perspect. 1994; 102(Suppl 9):157–167. [PubMed: 7698077]
2. Poland A, Knutson JC. Annu Rev Pharmacol Toxicol. 1982; 22:517–554. [PubMed: 6282188]
3. Whitlock JP Jr. Annu Rev Pharmacol Toxicol. 1999; 39:103–125. [PubMed: 10331078]
4. Ma Q. Curr Drug Metab. 2001; 2:149–164. [PubMed: 11469723]
5. Ma Q, Lu AY. Curr Drug Metab. 2008; 9:374–383. [PubMed: 18537574]
6. Ma, Q. The AH Receptor in Biology and Toxicology. Pohjanvirta, R., editor. John Wiley & Sons; Hoboken, New Jersey: 2012. p. 35-45.
7. Vasiliou V, Puga A, Chang CY, Tabor MW, Nebert DW. Biochem Pharmacol. 1995; 50:2057–2068. [PubMed: 8849333]
8. Ma Q, He X. Pharmacol Rev. 2012; 64:1055–1081. [PubMed: 22966037]
9. Talalay P. Biofactors. 2000; 12:5–11. [PubMed: 11216505]
10. Taguchi K, Motohashi H, Yamamoto M. Genes Cells. 2011; 16:123–140. [PubMed: 21251164]
11. Ma Q, Cui K, Xiao F, Lu AY, Yang CS. J Biol Chem. 1992; 267:22298–22304. [PubMed: 1385397]
12. Brunmark A, Cadenas E, Lind C, Segura-Aguilar J, Ernster L. Free Radic Biol Med. 1987; 3:181–188. [PubMed: 3117624]
13. Talalay P. J Biol Chem. 2005; 280:28829–28847. [PubMed: 15941714]
14. Favreau LV, Pickett CB. J Biol Chem. 1995; 270:24468–24474. [PubMed: 7592662]
15. Kensler TW, Wakabayashi N, Biswal S. Annu Rev Pharmacol Toxicol. 2007; 47:89–116. [PubMed: 16968214]
16. Ma Q. Annu Rev Pharmacol Toxicol. 2013; 53:401–426. [PubMed: 23294312]
17. Ma Q, Kinneer K, Bi Y, Chan JY, Kan YW. Biochem J. 2004; 377:205–213. [PubMed: 14510636]
18. Miao W, Hu L, Scrivens PJ, Batist G. J Biol Chem. 2005; 280:20340–20348. [PubMed: 15790560]
19. Shin S, Wakabayashi N, Misra V, Biswal S, Lee GH, Agoston ES, Yamamoto M, Kensler TW. Mol Cell Biol. 2007; 27:7188–7197. [PubMed: 17709388]
20. Ohtake F, Fujii-Kuriyama Y, Kato S. Biochem Pharmacol. 2009; 77:474–484. [PubMed: 18838062]
21. Miller AG, Israel D, Whitlock JP Jr. J Biol Chem. 1983; 258:3523–3527. [PubMed: 6300048]
22. Ma Q, Dong L, Whitlock JP Jr. J Biol Chem. 1995; 270:12697–12703. [PubMed: 7759522]
23. Dong L, Ma Q, Whitlock JP Jr. J Biol Chem. 1996; 271:7942–7948. [PubMed: 8626473]
24. Ko HP, Okino ST, Ma Q, Whitlock JP Jr. Mol Cell Biol. 1997; 17:3497–3507. [PubMed: 9199285]
25. Chan K, Lu R, Chang JC, Kan YW. Proc Natl Acad Sci USA. 1996; 93:13943–13948. [PubMed: 8943040]
26. Bianco NR, Chaplin LJ, Montano MM. Biochem J. 2005; 385:279–287. [PubMed: 15456407]
27. Favreau LV, Pickett CB. J Biol Chem. 1991; 266:4556–4561. [PubMed: 1900296]
28. Ma Q, Baldwin KT. J Biol Chem. 2000; 275:8432–8438. [PubMed: 10722677]
29. Nguyen T, Sherratt PJ, Pickett CB. Annu Rev Pharmacol Toxicol. 2003; 43:233–260. [PubMed: 12359864]

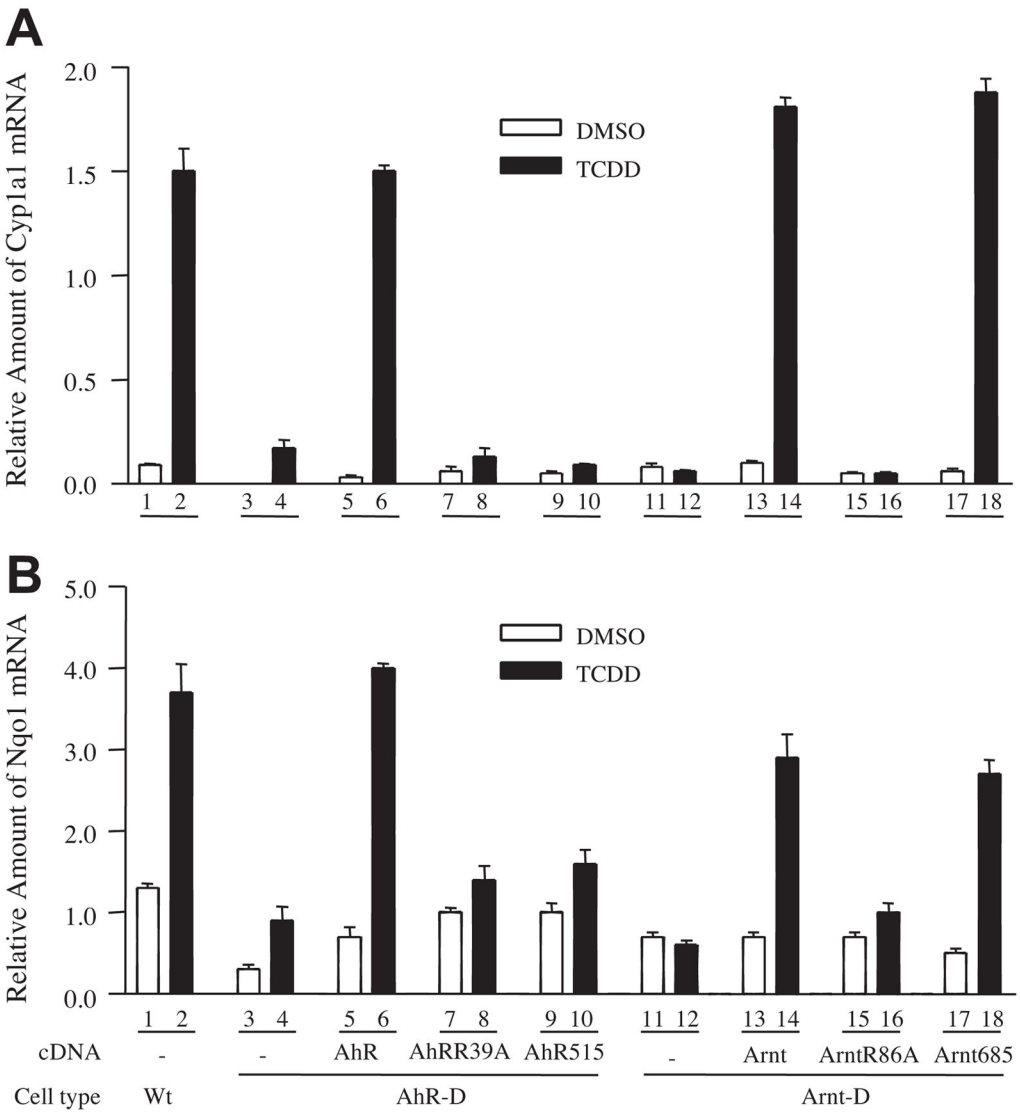

Fig. 1.

Induction of Cyp1a1 and Nqo1 by TCDD in hepa1c1c7 and variant cells. WT (hepa1c1c7), AhR-D, or Arnt-D cells and the variant cells reconstituted with AhR, Arnt, or their mutants were described under Material and Methods. Cells were grown to confluency and were treated with DMSO or TCDD (1 nM) for 4 h. Total RNA was analyzed for mRNA expression of Cyp1a1 (A) and Nqo1 (B) using real time-PCR. Relative amounts of cDNA were calculated from C_T values for each sample as described in Methods for real-time PCR. Data represents means ± standard deviations from triplet samples. The same experiments were repeated two more times with consistent results.

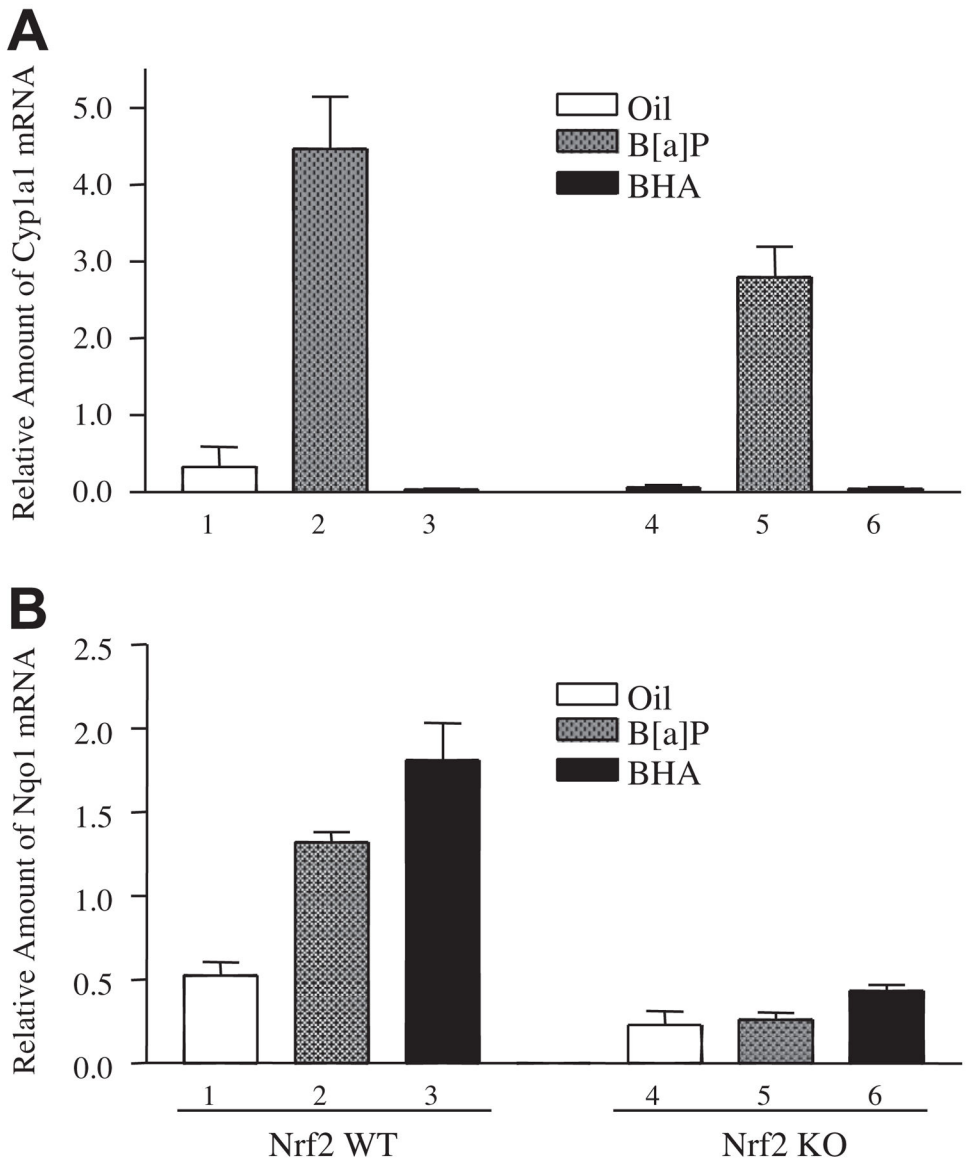

Fig. 2.

Induction of Cyp1a1 and Nqo1 in Nrf2 WT and KO mice. Adult Nrf2 WT and KO male mice in a C57BL/6 J background were treated with B[a]P or BHA as described under Material and Methods. Corn oil was used as vehicle control. Total RNA was prepared from the liver. Expression of Cyp1a1 (A) and Nqo1 (B) mRNAs was measured by real-time PCR as described for Fig. 1. Data represents means ± standard deviations from six RNA preparations from each genotype and treatment.

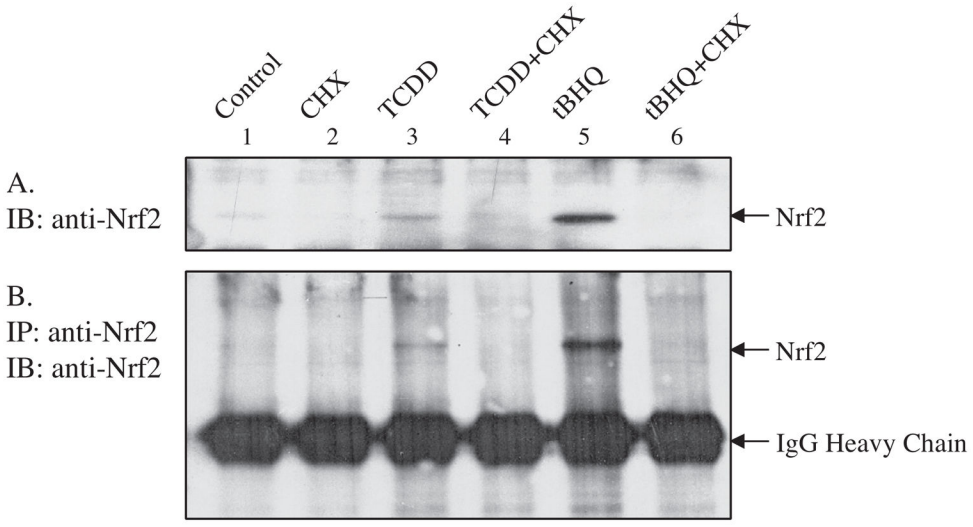

Fig. 3.

Stabilization of Nrf2 protein by TCDD. Hepa1c1c7 cells were grown to confluency in 10-cm plates and were treated with tBHQ (30 μM) or TCDD (1 nM) for 4 h. (A) Immunoblotting of Nrf2 in total cell lysate. (B) Immunoprecipitation of Nrf2. Cycloheximide (CHX) was used to inhibit Nrf2 protein synthesis. Antibodies used for IB and IP were described under Material.

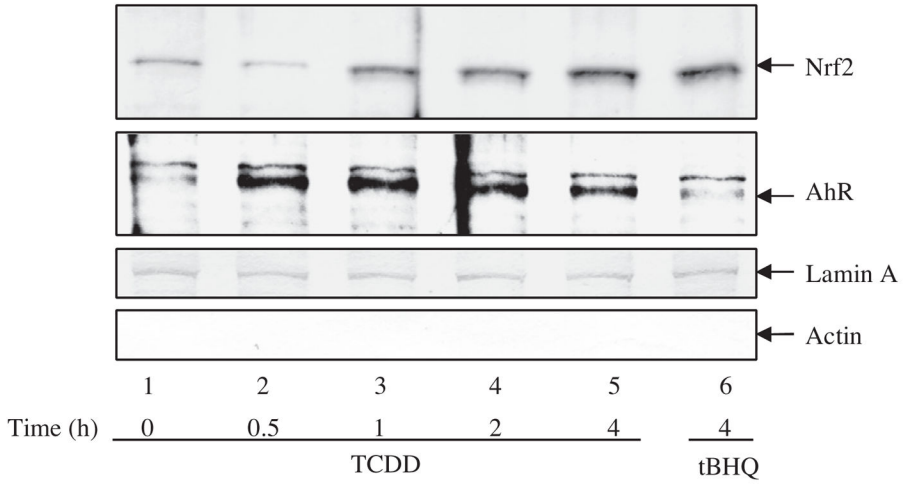

Fig. 4.

Nuclear localization of Nrf2 and AhR. Hepa1c1c7 cells were treated with TCDD (1 nM, 4 h). Nuclear extracts were prepared at indicated time points using the Nuclei EZ PREP reagents (Sigma). Treatment with tBHQ (30 μM, 4 h) was used a as a positive control for activation of Nrf2. Nrf2 and AhR were blotted using specific antibodies described under Material. Lamin A was used as a marker for nuclear fraction and Actin as a marker for cytoplasmic contamination.

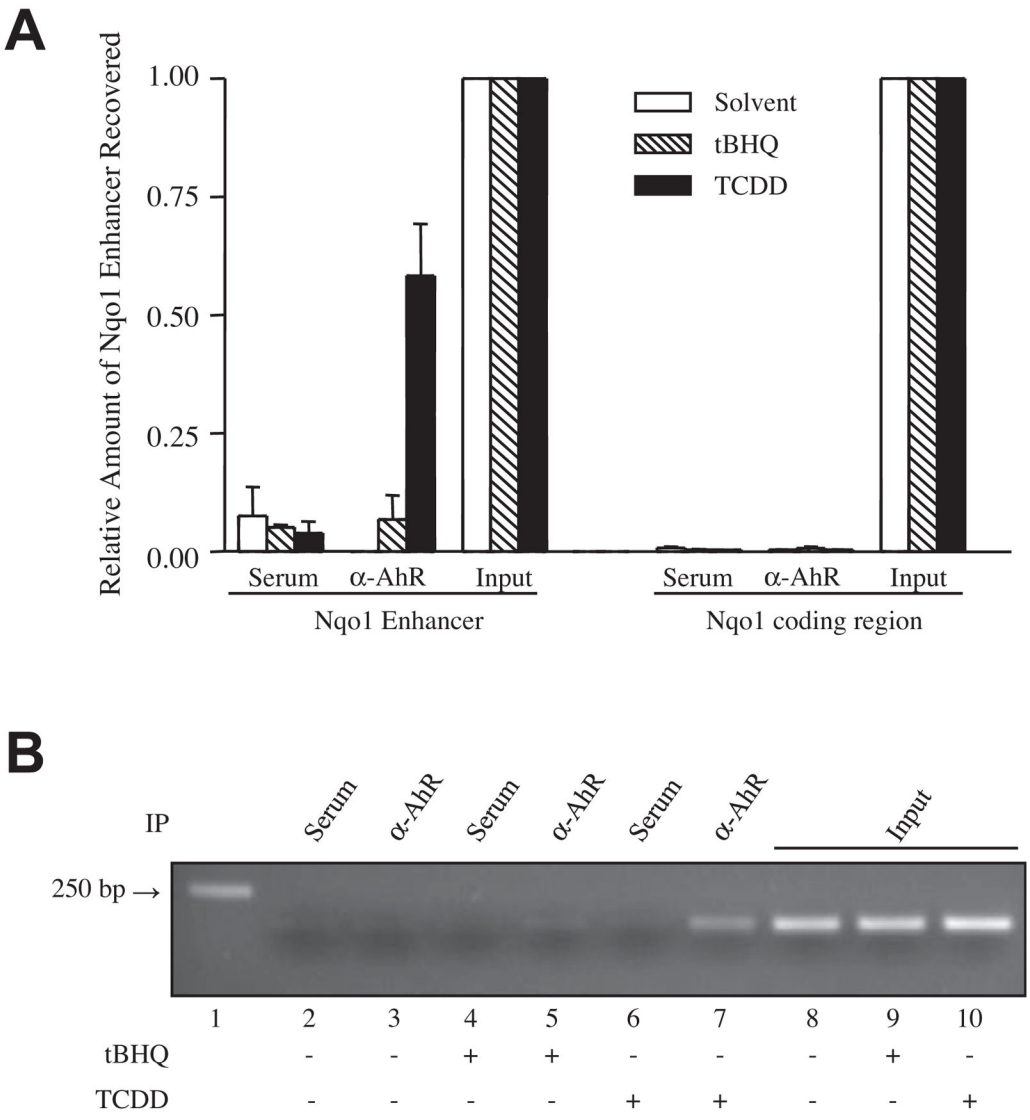

Fig. 5.

Binding of AhR to Nqo1 enhancer. Hepa1c1c7 cells were treated with TCDD (1 nM) or tBHQ (30 μM) for 4 h. ChIP assay was performed with anti-AhR antibodies to immunoprecipitate AhR-bound enhancer sequences. Specific DNA sequences were quantified by real-time PCR with primers specific for the ARE enhancer region or the coding region of Nqo1 (as a negative control) (A), or were amplified by real-time PCR and visualized on agarose gel (B). Quantitative data represents means ± standard deviations from three samples. The rabbit serum was used as the negative control for antibody and 10% of the input was included to show normalized input.

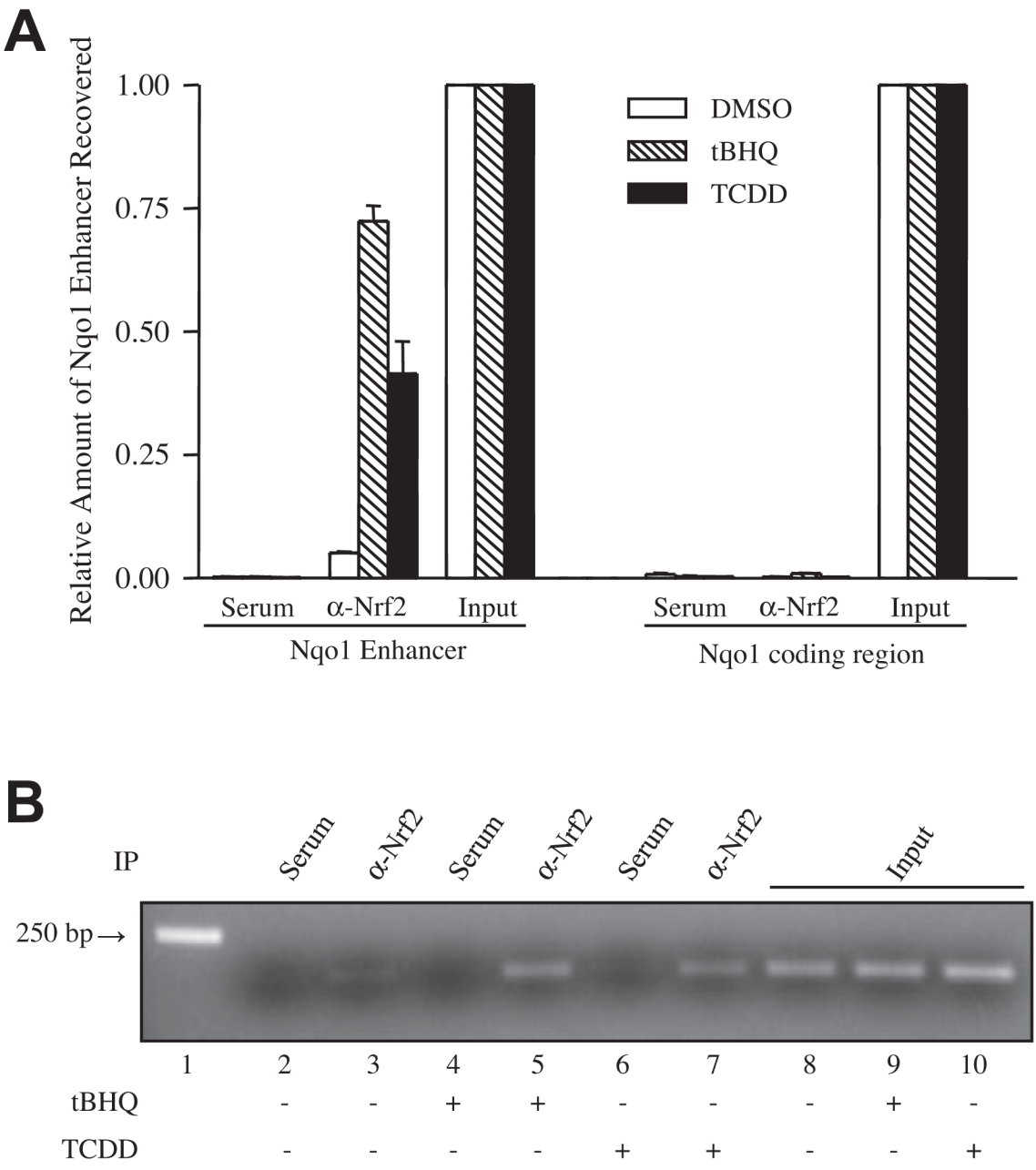

Fig. 6.

Binding of Nrf2 to Nqo1 enhancer. Hepa1c1c7 cells were treated with tBHQ (30 μM) or TCDD (1 nM) for 4 h. ChIP analysis was performed with anti-Nrf2 antibodies to immunoprecipitate Nrf2-bound enhancer sequences. Specific DNA sequences were quantified by real-time PCR with primers specific for the ARE enhancer region or the coding region of Nqo1 (as a negative control) (A), or were amplified by real-time PCR and visualized on agarose gel (B). Quantitative data represents means ± standard deviations from three samples. The rabbit serum was used as the negative control for antibody and 10% of the input was included to show normalized input.

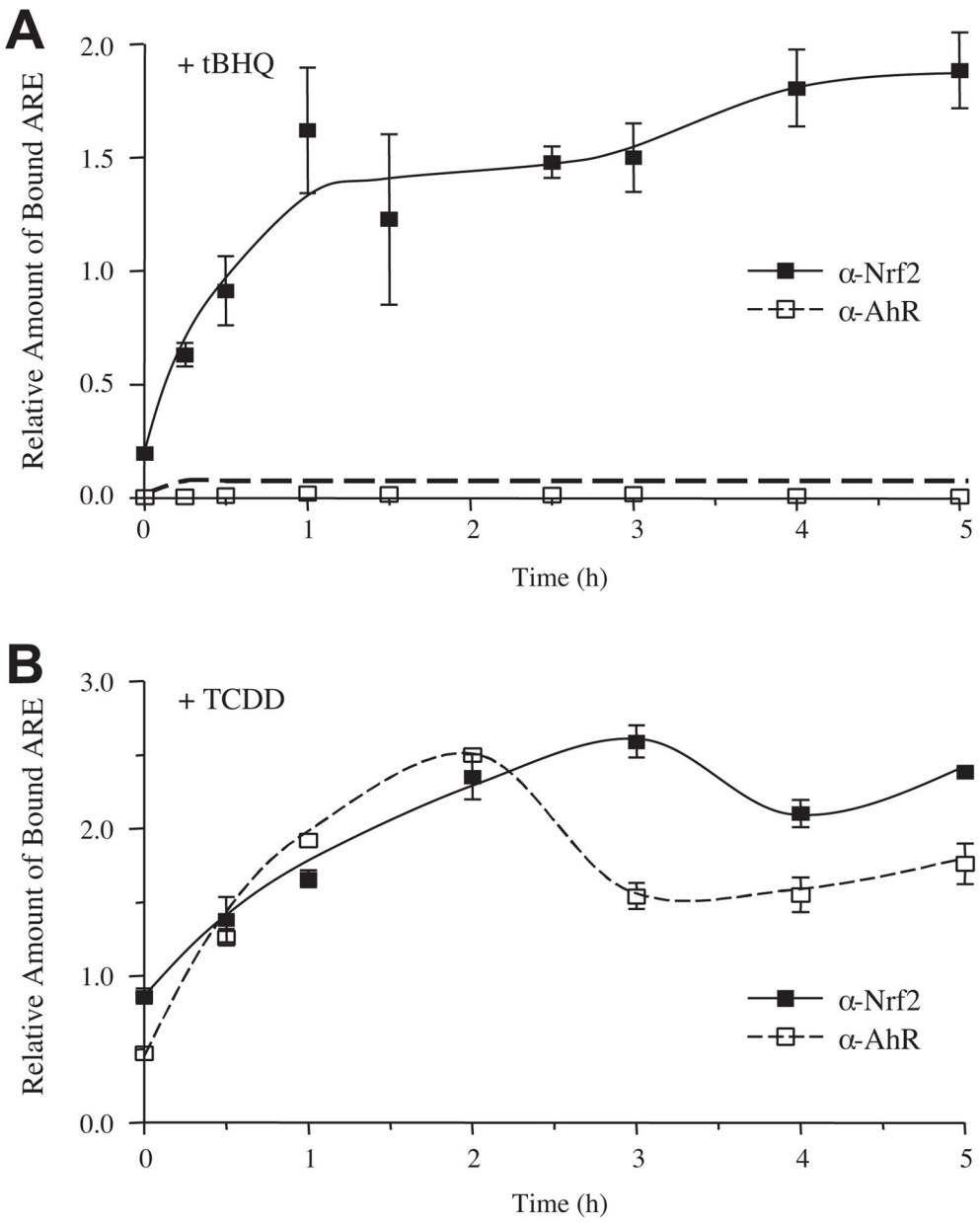

Fig. 7.

Time curves of tBHQ or TCDD-induced binding of Nrf2 and AhR to Nqo1 enhancer. Hepa1c1c7 cells were treated with tBHQ (30 μM) or TCDD (1 nM) for up to 5 h. ChIP was performed at indicated time points with antibodies against Nrf2 or AhR and real-time PCR was performed to amplify co-immunoprecipitated enhancer sequences. ChIP was performed using the protocol described under Material and Methods.

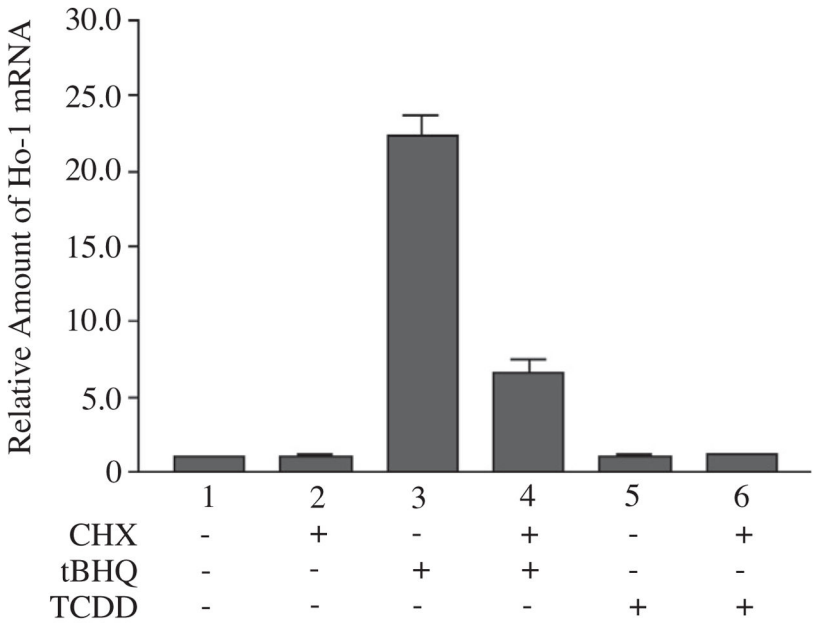

Fig. 8.

Effect of TCDD on Ho-1 expression. Hepa1c1c cells were treated with tBHQ (30 μM, 4 h, positive control); CHX (10 μg/ml, 4 h); TCDD (1 nM, 4 h), or combinations of the agents. Total RNA was prepared and expression of Ho-1 mRNA was examined by real-time PCR as described under Material and Methods. Results represent means ± standard deviations from triplicate samples. The same experiment was repeated twice with similar results.

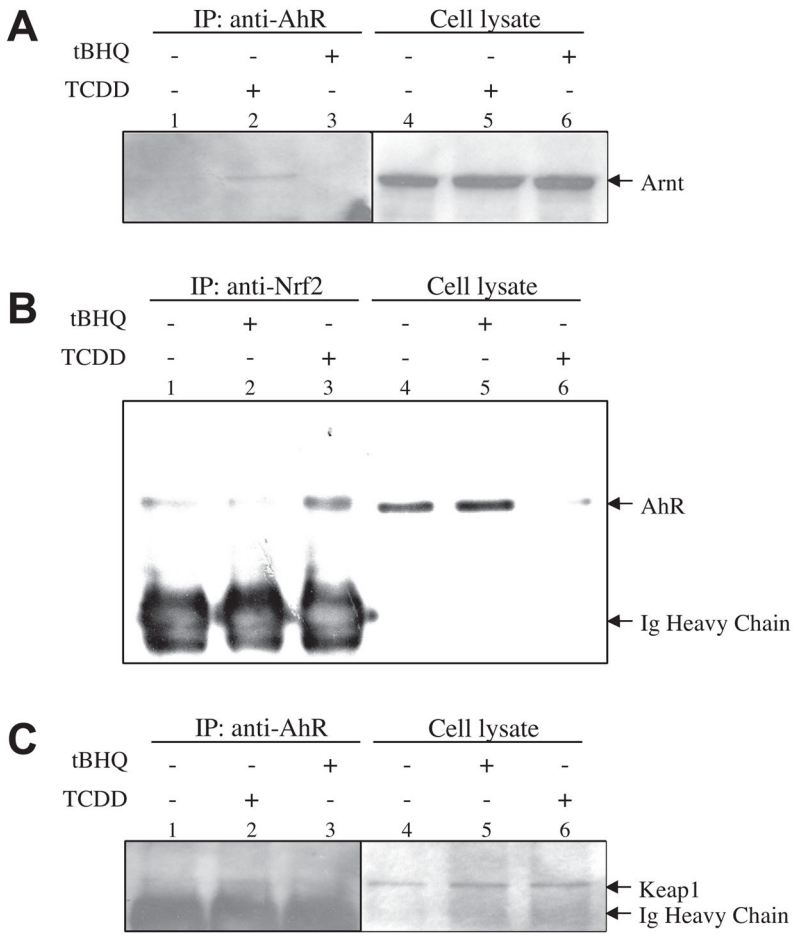

Fig. 9.

Interaction between AhR and Nrf2. Cells were treated with tBHQ (30 μM) or TCDD (1 nM) for 4 h. Cell lysate was prepared and immunoprecipitation was performed as described under Material and Methods. (A) AhR-Arnt interaction. (B) AhR-Nrf2 interaction. (C) AhR-Keap1 interaction.

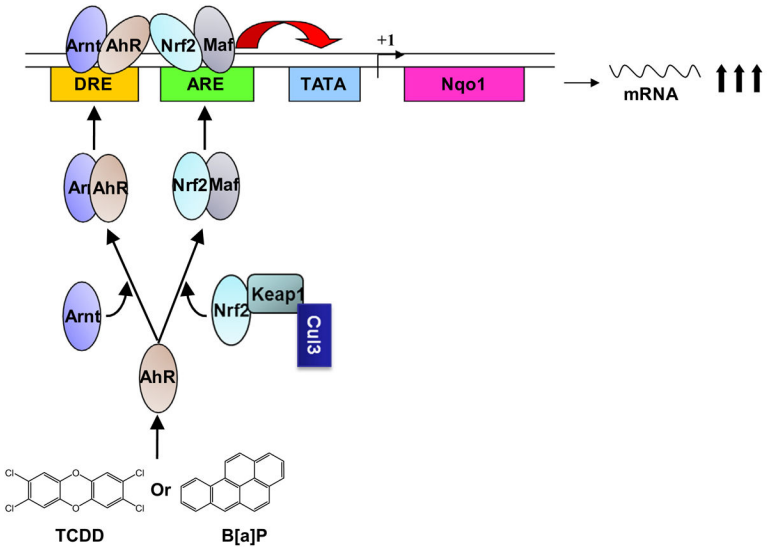

Fig. 10.

A working model of Nqo1 induction by AhR agonists. AhR agonists, such as TCDD and B[a]P, binds and activates AhR. Activated AhR translocates into the nucleus and dimerizes with Arnt in order to bind to DRE of the Nqo1 enhancer. Activated AhR also interacts with Nrf2, either directly or through the Nrf2/Keap1 complex, to inhibit Nrf2 degradation leading to Nrf2 nuclear accumulation, dimerization of Nrf2 with a small Maf, and increased binding of Nrf2/Maf to ARE. AhR may physically interact with Nrf2 at the enhancer. The concerted actions of AhR and Nrf2 are responsible for Nqo1 induction by AhR agonists.